In vivo activity of gemcitabine-loaded PEGylated small unilamellar liposomes against pancreatic cancer

**Donato Cosco · Alessandra Bulotta · Monica Ventura · Christian Celia ·
Teresa Calimeri · Gino Perri · Donatella Paolino · Nicola Costa · Paola Neri ·
Pierosandro Tagliaferri · Pierfrancesco Tassone · Massimo Fresta**

Abstract Gemcitabine (GEM) is presently the standard option for the treatment of advanced pancreatic cancer (PC). We investigated the in vitro and in vivo antitumor potential of GEM-loaded PEGylated liposomes (L-GEM) as a novel agent for the treatment of PC. In vitro analysis of antitumor activity against human PC cell lines, BXPC-3 and PSN-1, showed a significant time- and dose-dependent reduction of cell viability following exposure to L-GEM as compared to free GEM [at 72 h, IC$_{50}$: 0.009 vs. 0.027 μM ($P = 0.003$) for BXPC-3 and 0.003 vs. 0.009 μM ($P < 0.001$) for PSN1, respectively]. Confocal laser scanning microscopy demonstrated an effective liposome/cell interaction and internalization process following 3-h cell exposure to L-GEM. The in vivo antitumor activity of L-GEM was investigated in a cohort of SCID mice bearing BxPC-3 or PSN-1 xenografts. Animals were i.p. treated with L-GEM (5 mg/kg), or a threefold increased dose of free GEM (15 mg/kg), or empty liposomes or vehicle, twice a week for 35 days. A significant higher inhibition of tumor growth in mice treated with L-GEM versus free GEM ($P = 0.006$ and $P = 0.004$ for BXPC-3 and PSN-1, respectively) or control groups ($P = 0.0001$), translated in a survival advantage of L-GEM treated animals versus other groups. Pharmacokinetic studies showed enhancement of systemic bioavailability of L-GEM ($t_{1/2} = 8$ h) versus to GEM ($t_{1/2} = 1.5$ h). Our findings demonstrate that L-GEM is an effective agent against PC and exerts higher antitumor activity as compared to free GEM with no appreciable increase in toxicity. These results provide the pre-clinical rational for L-GEM clinical development for the treatment of PC patients.

D. Cosco and A. Bulotta contributed equally to this work.

In memory of Prof. Salvatore Venuta, MD, a victim of pancreatic cancer, an oncologist and a scientist who lived future frontiers of cancer therapeutics by strongly trusting in biomedical nanotechnologies.

D. Cosco · C. Celia · N. Costa · M. Fresta
Department of Pharmacobiological Sciences,
University "Magna Græcia", Campus Salvatore Venuta,
Catanzaro, Italy

A. Bulotta · M. Ventura · T. Calimeri · G. Perri · P. Neri ·
P. Tagliaferri · P. Tassone (✉)
Medical Oncology Unit and Referal Unit for Genetic
Counselling and Innovative Treatments,
Tommaso Campanella Cancer Center,
University "Magna Græcia", Campus Salvatore Venuta,
Viale Europa, 88100 Catanzaro, Italy
e-mail: tassone@unicz.it

D. Paolino · P. Neri · P. Tagliaferri · P. Tassone
Department of Experimental and Clinical Medicine G. Salvatore,
University "Magna Græcia", Campus Salvatore Venuta,
Catanzaro, Italy

List of abbreviations

AUC	Area under the curve
Chol	Cholesterol
CLSM	Confocal laser scanning microscopy
C_{max}	Maximum plasmatic concentration
DPPC	1, 2-Dipalmitoyl-*sn*-glycero-3-phospocholine monohydrate
DSPE-MPEG 2000	*N*-(Carbonyl-methoxypolyethylene glycol-2000)-1, 2-distearoyl-*sn*-glycero-3-phosphoethanolamine

EPR	Enhanced permeation and retention
Fluorescein-DHPE	N-(Fluorescein-5-tiocarbamoyl)-1, 2-dihexadecanoyl-sn-glycero-3-phosphoethanolamine triethylammonium salt
GEM	Gemcitabine—2^I, 2^I-difluorodeoxycytidine
HPLC	High performance liquid chromatography
L-GEM	Gemcitabine-loaded pegylated small unilamellar liposomes
PBS	Phosphate buffer saline solution
PC	Human pancreatic adenocarcinoma cancer
PEG	Poly-ethylene glycol
$t_{1/2}$	Plasma half-life
V_d	Volume of distribution

Introduction

Pancreatic cancer (PC) is one of the most aggressive tumors with only <4% of all patients surviving longer than 5 years after diagnosis [1]. Even if the surgical resection of the primary tumor may offer a chance of cure, most of patients recurs or are not resectable at time of diagnosis, due to the very early local aggressiveness. Locally advanced or metastatic PC patients have a very poor prognosis. To date, systemic chemotherapy, based on the nucleoside analog gemcitabine ($2^I,2^I$-difluorodeoxycyti-dine) (GEM), is the mainstay of palliative treatment, improving the disease-related symptoms and producing an objective response rate of <20%.

The mechanism of action of GEM is based on its progressive intracellular phosphorylation up to the formation of the triphosphate derivative, which acts as a false nucleotide being incorporated in the DNA chain. In addition, both diphosphate and triphosphate GEM nucleotides are able to inhibit the ribonucleotide reductase, thus eliciting a reduction of the concentration of deoxynucleotides necessary for DNA synthesis. These combined actions lead to the inhibition of DNA synthesis and the arrest of cell proliferation in S-phase [2]. Under the biopharmaceutical point of view, GEM is rapidly converted into the inactive metabolite 2^I-deoxy-$2^I,2^I$-difluorouridine by cytidine deaminase following systemic infusion and the inactive metabolite is excreted in the urine [3]. The very short plasma half-life (8–17 min) partially explains the low systemic activity of GEM [4].

Accumulating body of evidence supports the idea that drug entrapment in liposomes is a successful strategy to overcome limitations of drug pharmacokinetics and to

avoid rapid metabolic inactivation [5, 6]. Liposomes, which are the archetypal and the most biocompatible and bio-mimetic form of drug nanovectors, may significantly improve the drug activity taking benefit from the slow vascular and extravascular flow in the tumor and from the leaky cancer neovasculature [7]. In fact, the presence of large fenestrations in tumor vessels significantly enhances permeability and allows local retention of liposomal nanovectors [enhanced permeation and retention (EPR) effect] with the final goal of an efficient passive targeting and increased therapeutic effects. In particular, the reduction of liposomal size (<200 nm) and the decrease of the surface charge by means of liposome coating with uncharged highly hydrophilic polymers, i.e., poly-ethylene glycol (PEG) (PEGylated liposomes), improve the systemic carrier half-life with the advantage of a better bioavailability at tumor site and the reduction of side effects, as in the case of Doxorubicin-loaded PEGylated liposomes (Doxil®) [8–10]. Even though more sophisticated active targeting strategies have been proposed for cancer therapy [11, 12], the passive targeting, based on the EPR effect, and the PEGylation of colloidal carrier, is already a reliable and clinically effective strategy [13, 14]. However, an extensive investigation on the passive targeting of vesicular colloidal carriers by pegylation is still needed to study the potential therapeutic role of this approach in cancer treatment.

Aim of this study is the investigation of in vitro and in vivo effects induced by gemcitabine-loaded PEGylated small unilamellar liposomes (L-GEM) against human PC cell lines and human xenografts as compared to free GEM. The interaction of liposomal vectors with the human PC cells was also investigated by means of confocal laser scanning microscopy (CLSM) and the in vivo pharmacokinetic profiles of both free GEM and L-GEM was assessed.

Materials and methods

Chemicals and biochemicals

Cholesterol (Chol), phosphate buffer saline solution (PBS), N-(fluorescein-5-tiocarbamoyl)-1,2-dihexadecanoyl-sn-glycero-3-phosphoethanolamine triethylammonium salt (fluorescein-DHPE), 3-[4,5-dimethylthiazol-2-yl]-3,5-diphenyltetrazolium bromide salt (tetrazolium salt), RPMI 1640 media, fetal bovine serum, 2 mM L-glutamine, 100 U/ml penicillin, 100 µg/ml streptomycin were obtained from Sigma Chemicals Co. (St. Louis, USA). 1,2-dipalmitoyl-sn-glycero-3-phospocholine monohydrate (DPPC) and N-(carbonyl-methoxypolyethylene glycol-2000)-1,2-distearoyl-sn-glycero-3-phosphoethanolamine (DSPE-MPEG

2000) were purchased from Genzyme (Suffolk, UK). Sterile saline was a product of Frekenius Kabi Potenza S.r.l. (Verona, Italy). The human pancreatic adenocarcinoma cancer cell lines BxPC-3 and PSN-1 were purchased from the Cell Bank of the National Institute for Cancer Research (Genova, Italy). Gemcitabine (2′,2′-difluorodeoxycytidine) hydrochloride (HPLC purity >99%) was obtained from Eli-Lilly Italia S.p.A. (Sesto Fiorentino, Florence, Italy) and it was used without further purification. All other chemical reagents used in this investigation were of analytical grade (Carlo Erba, Milan, Italy).

GEM stability in the culture medium was assessed by repeated HPLC analysis.

Liposome preparation

Liposomes were made up of DPPC/Chol/DSPE-MPEG2000 (6:3:1 molar ratio) and were prepared and characterized as reported elsewhere [15]. Briefly, lipid mixture (20 mg) was dissolved in a round-bottomed flask by using a chloroform/methanol (3:1 v/v) solvent mixture, which was removed by means of a rotary evaporator (Büchi R-210 Switzerland) and by an overnight storage at room temperature in a Büchi T51 glass drying oven connected to a vacuum pump, thus allowing the formation of a thin layer lipid film. When required, fluorescent labeled liposomes were prepared by co-dissolving fluorescein-DHPE (0.1% molar) with the lipids. Lipid films were hydrated with a 250 mM ammonium sulfate solution (1 ml) and then submitted to ten cycles of freezing (with liquid nitrogen) and thawing (with a water bath at 40°C), thus achieving a pH gradient with a homogenous acid environment in the intra-liposomal aqueous compartments. Multilamellar vesicles were submitted to extrusion through 400, 200 and 100 nm pore size two stacked polycarbonate filters (Costar, Corning Incorporated, NY, USA) by using a stainless steel extrusion device (Lipex Biomembranes, Vancouver, BC, USA) and un-entrapped ammonium sulfate solution was removed by centrifugation. Small unilamellar colloidal vesicles were suspended in an isotonic solution (1 ml) of GEM-hydrochloride (1 mM) and kept at room temperature for 3 h. The unentrapped drug was removed by gel permeation chromatography thus obtaining L-GEM. The liposome encapsulation efficiency was calculated as a percentage with respect to the amount added during preparation. Liposomes were physico-chemically characterized by light scattering.

Physicochemical characterization of liposomes

Mean size and size distribution (polydispersity index) of L-GEM were evaluated by dynamic light-scattering experiments. Zetamaster (Malvern Instruments Ltd.,

Spring Lane South, Worcs, UK), a photo-correlation spectroscopy apparatus, was used for the dimensional analysis. Zetamaster is equipped with a 4.5-mW laser diode operating at 670 nm. Experiments were carried out at a scattering angle of 90°. A third-order cumulant fitting correlation function was performed by a Malvern PCS sub-micron particle analyzer to obtain mean size and polydispersity index of L-GEM. A medium refractive index of 1.330, a medium viscosity of 1.0 mPa s and a dielectric constant of 80.4 were set as instrumental parameters for light-scattering experiments. Samples were suitably diluted with a filtered (Sartorius membrane filters 0.22 μm) saline to avoid multiscattering phenomena and placed in a quartz cuvette. Experiments were carried out at room temperature.

Tissue culture

PC cells BxPC-3 and PSN-1 were grown in RPMI 1640 media (Sigma Aldrich, Italy) supplemented with 10% fetal bovine serum (Sigma), 2 mM L-glutamine (Sigma), 100 U/ml penicillin (Sigma), and 100 μg/ml streptomycin (Sigma). The two PC cell lines were cultured in plastic culture dishes (100 mm × 20 mm) at 37°C in a humidified atmosphere with 5% CO_2. Cultures were free of *Mycoplasma* and pathogenic murine viruses and were maintained for no longer than 8 weeks after recovery from frozen stocks (liquid nitrogen). When a ~80% confluence was reached, cells were trypsinized (2 ml) and collected into a centrifuge tube containing 4 ml of the culture medium. The dishes were further washed with 2 ml of PBS to remove the remaining cells and then the washing buffer was transferred into the centrifuge tube, which was centrifuged at 1,000 rpm at room temperature for 10 min (Megafuge 1.0, Heraeus Sepatech, Osterode/Harz, Germany). The pellet was resuspended in a suitable volume of culture medium and seeded in culture dishes before in vitro investigations.

In vitro studies

Cell proliferation assays

To assess cellular cytotoxicity the MTT test was carried out. PSN-1 (5×10^3/well) and BxPC-3 (7.5×10^3/well) cells were seeded in 96-well tissue culture plates for 24 h at 37°C, thus allowing cell adhesion to culture plates. Culture medium was removed and replaced with fresh medium containing free or liposomally entrapped GEM at different concentrations (evaluation of the dose-dependent activity) and cells were then incubated for 48 or 72 h. Every plate had 8 wells with untreated cells as

the control and 8 wells with cells treated with empty liposomes as the blank. In this case, empty liposomes underwent to the same dilution of L-GEM. After each incubation period, 10 μl of tetrazolium salt solubilized in PBS solution (5 mg/ml) was added to each well and the plates were incubated at 37°C for 3 h. The medium was then removed and the formazan salts were dissolved with 200 μl of a solution of ethanol/DMSO (1:1 v/v) by shaking plates for 20 min at 230 rpm (IKA® KS 130 Control, IKA® WERKE GMBH & Co., Staufen, Germany). The sample absorbance was measured by means of a microplate reader (LabSystems Multiskan MS M-Medical, Italy) at a wavelength of 540 nm with reference at a wavelength of 690 nm. The percent cell viability was calculated according to the following equation:

$$\text{cell viability} = \text{Abs}_T / \text{Abs}_C \times 100 \tag{1}$$

where Abs_T is the absorbance of treated cells and Abs_C is the absorbance of control (untreated) cells. The formazan concentration is directly proportional to the cell viability. Data on cell viability are reported as the mean of six different experiments ± standard deviation.

Confocal laser scanning microscopy (CLSM) experiments

The interaction between PC cells and liposomes was evaluated by CLSM. Cells were placed in 6-well culture plates (4×10^5 cells/ml) with culture medium. In each well a sterile glass slide was previously positioned. Plates were incubated for 24 h and then cells were treated with liposomes labeled with fluorescein-DHPE for different incubation times, from 3 h up to 24 h. After incubation, each well was washed with PBS (3 times) to remove the excess of vesicles and cells were fixed on the sterile glass slides by using 1 ml of an ethanolic solution (70% v/v). Each slide glass was washed again with PBS three times and PBS (2 ml) was added to each well. Plates were stored at 4°C up to the confocal microscopy analysis. Before analysis, slide glasses were positioned on cover-glass by using a glycerol solution (70% v/v) to remove enclosed air and they were fixed by a transparent glue. The analysis was carried out using a Leika TCS SP2 MP laser scanning confocal microscope at a $\lambda_{exc} = 496$ nm and a $\lambda_{em} = 519$ nm. A scan resolution up to $4,096 \times 4,096$ pixels with an Ar/Kr laser beam of 75 mW, equipped with a fluorescein analyzer filter, was used for experimental investigations. Samples were recorded by a macro developer software package having multi-dimensional series acquisition and direct-access digital control knobs. An immersion oil lens $100\times$ was used.

In vivo studies

Human PC xenograft models

CB-17 SCID-mice were purchased from Charles River (France), maintained and monitored in our animal research facility. Care and handling of animals were in accordance with the Italian low.

Mice were subcutaneously (s.c.) inoculated in the interscapular area with 3×10^6 and 2.5×10^6 PSN-1 and BxPC-3 cells (100 μl in RPMI-1640 medium), respectively. When the tumor was measurable, approximately 2 and 3 weeks after PSN-1 or BxPC-3 cell injection, respectively, mice were i.p. treated with L-GEM (5 mg/kg, $n = 5$ mice), a threefold increased dose of free GEM (15 mg/kg, $n = 5$), empty liposomes ($n = 5$) or isotonic saline solution (NaCl 0.9% w/v, $n = 5$), twice a week for 35 days. GEM dose and schedule used here have been chosen according to other reports where GEM as been used at doses in a range between 7.5 and 15 mg/kg weekly or twice weekly [16, 17]. GEM and L-GEM concentrations used in our study are below MTD which has been found at significant higher dose (approximately 200 mg/kg). Tumor size was measured every 4 days in two dimensions using an electronic caliper, and the tumor volume was calculated using the following formula:

$$V = 0.5ab^2 \tag{2}$$

where a and b are the long and short diameter of the tumor, respectively. To avoid unnecessary sufferance, animals were killed when their tumors reached 2 cm in diameter. Survival was calculated from the first day of treatment until the day of killing. Detailed procedure of in vivo studies has been previously reported [18, 19].

Pharmacokinetic studies

CB-17 SCID-mice (1 month old, 25 g) were used for pharmacokinetic studies. Free GEM or L-GEM (1 mg/ml) were injected (100 μl) through the tail vein (groups of five animals). Blood samples (200 μl) were taken from the tail vein at various times and refrigerated. Then, defrost samples were immediately centrifuged (10 min, 12,000 rpm) at room temperature and acetic acid (50 μl) was added to plasma samples to decrease hydrogen bonding between nucleosides and proteins. Acetonitrile (1 ml) (HPLC grade) was added to plasma samples, that were vortex-mixed and then centrifuged at $800g$ for 15 min at 4°C. The supernatant was removed and collected in a glass tube and acetonitrile (1 ml) was added to the pellet. Three cycles of vortex-mixing and centrifugation procedure were carried out. Supernatants were combined and evaporated to dryness under nitrogen flux at 42°C (thermostated water bath) and stored at −20°C.

Before the HPLC analysis, the residue was resuspended in water (1 ml) (HPLC grade), incubated for 5 min at 37°C and then centrifuged at 12,000g for 10 min at 20°C. The supernatant was removed, filtered through a 0.22 μm pore size Anotop 10 syringe filter (Whatman, Springfield Mill, UK) and placed in 4-ml HPLC glass vials for the analytical determination. Analysis was performed by using an HPLC system (Varian Inc., Palo Alto, USA) consisted of a 200-2031 Metachem online degasser, a M210 binary pump, a ProStar 410 autosampler, a G1316A thermostated column compartment, a 25 μl CSL20 Cheminert Sample Loop injector. Data were acquired and processed with a Galaxie® chromatography manager software (Varian Inc., Palo Alto, USA). Chromatographic separation was carried out at room temperature by using a GraceSmart RP C18 column (4.6 × 250 mm, 5 μm particle size, Alltech Grom GmbH, Rottenburg-Hailfingen, Germany). The mobile phase consisted of deionized water (HPLC grade) and acetonitrile (HPLC grade) 95:5 v/v. The flow rate was 1 ml/min and UV detection was performed at 269 nm.

No interference was observed for GEM and its metabolite, 2′,2′-difluorodeoxyuridine, HPLC peaks due to any plasma component. The chromatographic method provided a suitable separation of the peaks of GEM and its metabolite (2′,2′-difluorodeoxyuridine), which showed a retention time of 6 and 8.70 min, respectively. The GEM quantification was carried out by using an external standard curve in the linear concentration range between 0.1 and 10 μg/ml. A standard solution of GEM (1 mg/ml) was used for the construction of the standard curve. Plasma amount of GEM were determined using the standard curve according to the following equation:

$$AUC = 0.60112x + 0.02840 \tag{3}$$

where x is the drug concentration (μg/ml) and AUC the area under the curve (mAu × min).

GEM plasma amount were expressed as μg/ml. Experimental data are the mean of three different experiments.

Statistical analysis

One-way ANOVA and Student t-test was used for statistical analysis of the experimental date. A posteriori Bonferroni t-test was carried out to check the ANOVA test. A P-value <0.05 was considered statistically significant. Values are reported as the mean ± standard deviation.

Results

The pH-gradient method used for L-GEM preparation allowed an effective drug entrapment as high as 88.5% with respect to the amount added during the preparation procedure, in agreement with our previous results [15]. These findings demonstrated the suitability of liposomes as potential drug carrier for GEM. Taking into account the great relevance in terms of biopharmaceutical features of the mean size and size distribution of a colloidal carrier as a suitable drug delivery system for anticancer treatment, PEGylated liposomes underwent to an extrusion procedure thus producing a mean vesicular size of 136 ± 14 nm with a polydispersity index of 0.12 (highly homogenous size distribution).

In vitro activity of L-GEM against PC cell lines

We first investigated the in vitro antitumor activity of L-GEM against BxPC-3 and PSN-1 PC cells by MTT assay. As shown in Fig. 1, L-GEM induced a significant dose-dependent reduction of the cell viability as compared to free GEM. A lower IC_{50} value of L-GEM versus the free drug was achieved: at 72 h, the IC_{50} value L-GEM was significantly ($P < 0.001$) lower as compared to the free GEM for both cell lines (0.009 vs. 0.027 μM for BXPC-3 and 0.003 vs. 0.009 μM for PSN1, respectively) (Table 1). A physical mixture of free GEM and empty liposomes was also tested to evaluate the real advantage of the drug encapsulation. This mixture did not show any improvement in terms of antitumor activity as compared to the free drug (data not shown). Vehicle or empty liposomes did not affect cell survival of both BxPC-3 and PSN-1 lines (data not shown).

Liposome–cell interaction

An important step of our research was the study of the interaction between the liposomal carrier and the biological substrate. A liposome formulation labeled with fluorescein-DHPE was used for CLSM studies. Liposome/cell interaction was evaluated after 3, 6, 12 and 24 h of incubation. To evaluate the occurrence of artefacts due to the basal fluorescence of the cellular components, control samples were observed both in transmission mode (Figs. 2a, 3a) and after exposition at the fluorescein excitation wavelength (Figs. 2b, 3b). No significant fluorescent emission was observed, suggesting the absence of fluorescence interference phenomena. Following 3 h incubation (Figs. 2c, 3c), cell membranes were stained by vesicular carriers. The photomicrograph in Fig. 3c shows the presence of liposomes on the cell surface of BxPC-3 cells. Following 24 h, intracytoplasmic localization of vesicular carriers (Figs. 2, 3f) was detected.

In vivo antitumor activity

We next evaluated the in vivo antitumor activity of L-GEM by two xenograft murine models of human PC. A cohort of

Fig. 1 In vitro dose and time-dependent antitumor effects induced by GEM (*filled circles*) and L-GEM (*filled triangles*) on PSN-1 and BxPc-3 cells. Analysis was performed by MTT assay. Data are reported as percentage of control (untreated cells). Results are the mean of six different experiments ± standard deviation. Statistical analysis was performed by one-way ANOVA and a posteriori Bonferroni *t*-test: $*P < 0.05$; $**P < 0.001$
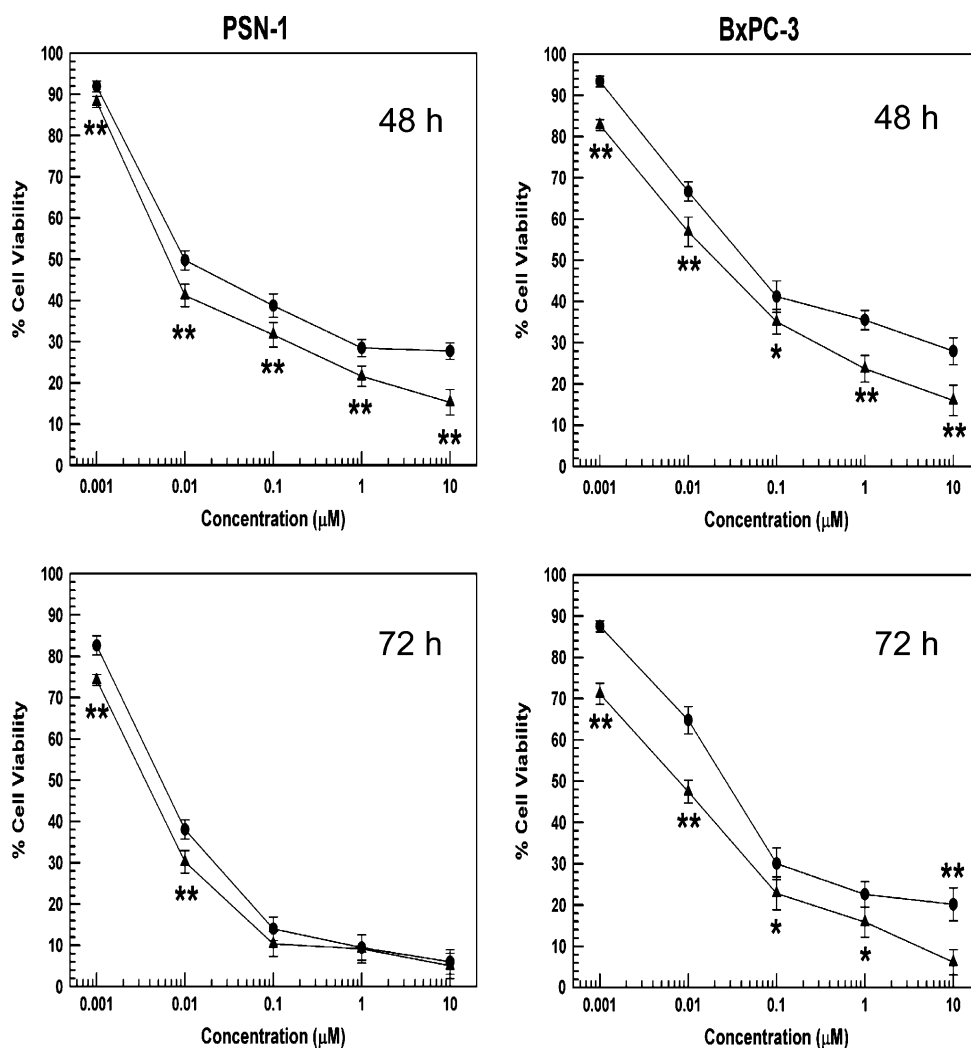
Table 1 IC_{50} values (μM) of free GEM and L-GEM after 48 and 72 h treatment of PC cells

	48 h		72 h	
	PSN-1	BXPC-3	PSN-1	BXPC-3
GEM	0.009 ± 0.0008	0.048 ± 0.006	0.009 ± 0.001	0.027 ± 0.005
L-GEM	0.006 ± 0.0004	0.021 ± 0.004	0.003 ± 0.0008	0.009 ± 0.0006
P-value	0.005	0.002	0.001	0.003

40 SCID mice bearing s.c. PSN-1 (20 mice) or BxPC-3 (20 mice) human xenografts were respectively i.p. treated with L-GEM (5 mg/kg, $n = 5$ mice), with a the threefold increased dose of free GEM (15 mg/kg, $n = 5$ mice), with empty liposomes ($n = 5$) or vehicle ($n = 5$), twice a week for 35 days. It is important to consider that a wide range of GEM concentrations has been previously reported [16, 17, 20, 21]. These differences can be explained by (1) intrinsic sensitivity of different tumor cell lines to the drug, (2) different in vivo models, (3) different drug bioavailability in different mouse strains. As shown in Fig. 4, a significant tumor growth inhibition was detected in animals treated with L-GEM or GEM versus control groups. Specifically, L-GEM induced higher growth inhibition as compared to free GEM ($P = 0.006$) and a significant survival advantage (20 days; $P = 0.03$) of mice bearing BXPC-3 xenografts (Fig. 4b, d). In parallel, L-GEM showed a significantly higher tumor growth inhibition versus free GEM in PSN-1 tumor xenografts ($P = 0.004$). Also in this case, the survival of L-GEM-treated animals was longer than free drug-treated mice (77 vs. 61 days; $P = 0.02$) (Fig. 4a, c).

These findings clearly indicate that L-GEM exerts more effective antitumor activity than the free drug, even if L-GEM has been used at a threefold lower concentration.

Fig. 2 Confocal laser scanning micrographs showing the interaction between L-GEM and PSN-1 cells. The time-dependent intracellular localization of fluorescein-DHPE labeled liposomes is shown. **a** and **b** are controls (untreated cells): in **a** cells are observed in transmission mode, in **b** no significant cellular fluorescence was observed from the autofluorescent phenomena caused by the cellular components. **c**, **d**, **e** and **f** (treated cells) after 3, 6, 12 and 24 h, respectively
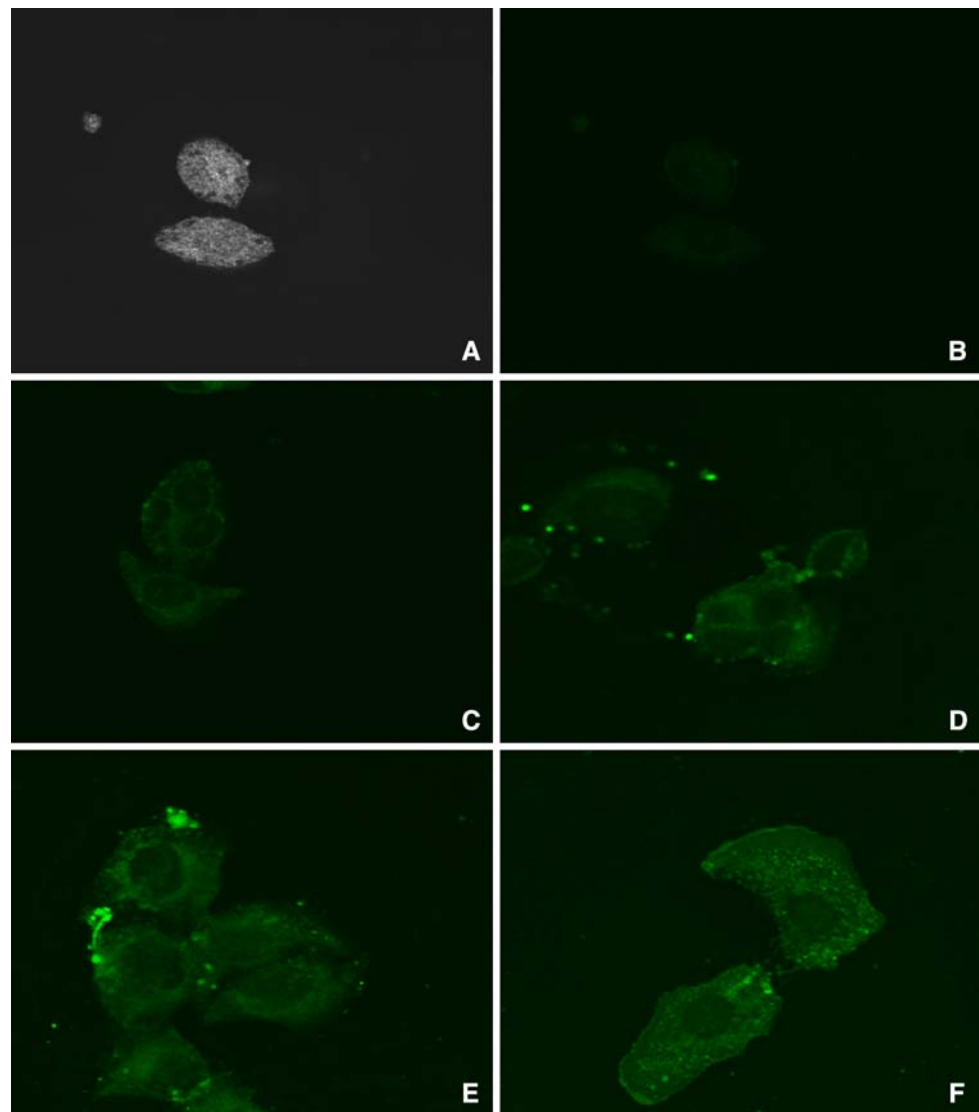
Importantly, by both formulations, we did not observe any toxicity including weight loss or other signs related to compromise of quality of life nor sudden death at used concentrations.

Pharmacokinetic studies

Plasma concentration profiles of free GEM and L-GEM and a summary of the major pharmacokinetic parameters were reported in Fig. 5 and Table 2, respectively. Differences in pharmacokinetic properties of GEM and its metabolite, 2′,2′-difluorodeoxyuridine, were observed. GEM disappeared rapidly from plasma (Fig. 5) due to the metabolic conversion into 2′,2′-difluorodeoxyuridine metabolite [22–24]. Pharmacokinetic profiles showed a biphasic pattern of the drug both in the free and liposomal formulation. The maximum plasmatic concentration (C_{max}) of GEM was 0.55 µg/ml at 0.5 h following the intravenous administration. The plasma concentration of GEM declined rapidly after 1 h of infusion. The GEM half-life ($t_{1/2}$) was 1.5 h with a measured plasma drug concentration of 0.26 µg/ml (Table 2). A different behavior was observed for the GEM metabolite, 2′,2′-difluorodeoxyuridine. In fact, the C_{max} of 2′,2′-difluorodeoxyuridine was 1.25 µg/ml at 1 h after the administration and the half-life was reached after 4 h. The pharmacokinetic profile of 2′,2′-difluorodeoxyuridine declined by a similar shape observed for the native drug. However, a constant 2′,2′-difluorodeoxyuridine plasma concentration was followed by a gradual decrease at 1–2 h. These findings evidenced that GEM and its inactive metabolite had a similar plasmatic distribution, but the metabolite was still present in the plasma after 20 h (Fig. 6).

Significant differences in the pharmacokinetic profile and parameters were observed when GEM was entrapped in liposomes. In fact, L-GEM was slowly removed from

Fig. 3 Confocal laser scanning micrographs showing the interaction between L-GEM and BXPC-3 cells. The time-dependent intracellular localization of fluorescein-DHPE labeled liposomes is shown. **a** and **b** are controls (untreated cells): in **a** cells are observed in transmission mode, in **b** no significant cellular fluorescence was observed from the autofluorescent phenomena caused by the cellular components. **c**, **d**, **e** and **f** (treated cells) after 3, 6, 12 and 24 h, respectively
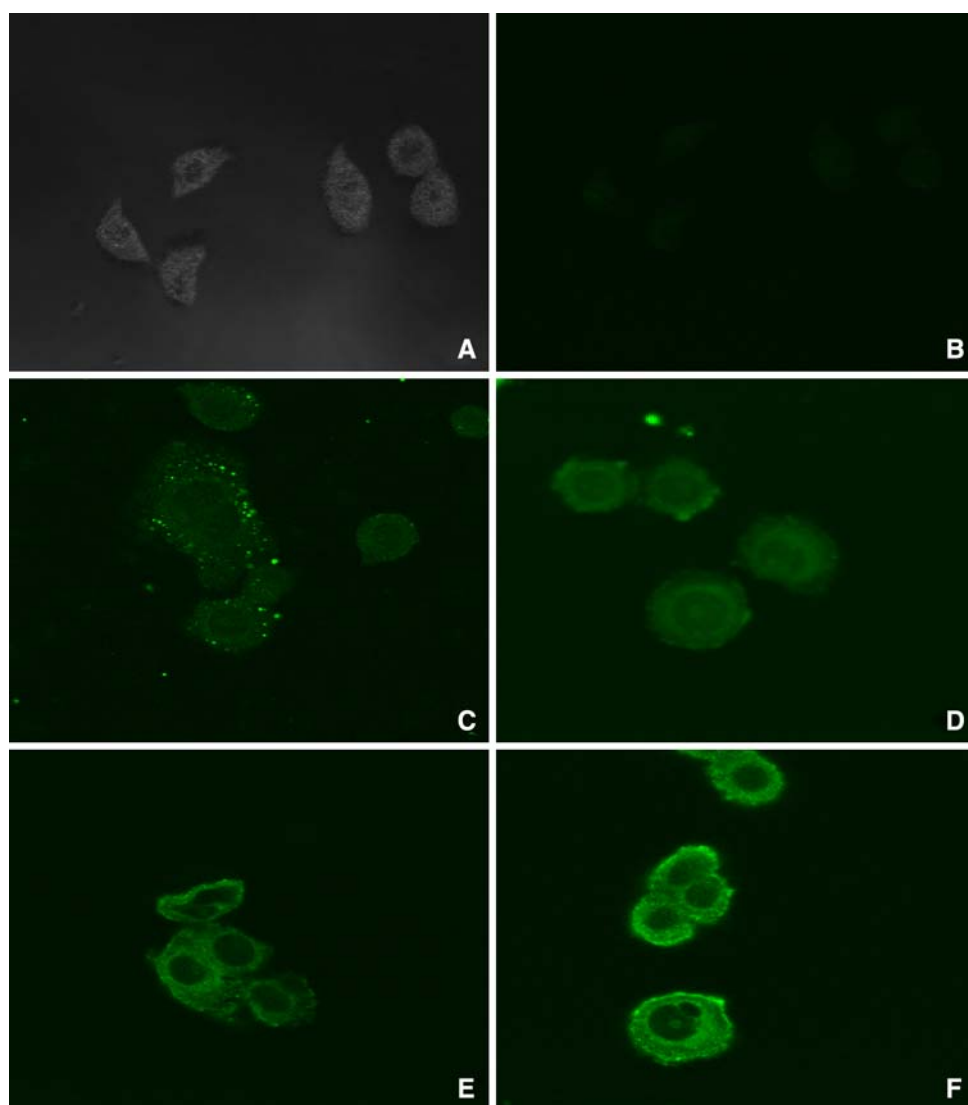
blood circulation following intravenous administration (Fig. 5). A C_{max} of ~ 0.52 μg/ml was obtained at 2 h after the infusion and the plasma drug concentration remained elevated (~ 0.2 μg/ml) up to 16 h with respect to the un-entrapped GEM, which was no more detectable after 2 h from the infusion. The $t_{1/2}$ of L-GEM was 8 h (Table 2). These findings were also supported by the evaluation of the volume of distribution (V_d) and area under the curve (AUC) parameters (Table 2). In fact, V_d value of L-GEM (444.44 ml) was 2.5-fold higher than that of GEM (181.81 ml), probably due to the rapid enzymatic inactivation of the drug, while the AUC value of L-GEM (5.171 μg/ml) showed an improvement of 7.5-fold with respect to free GEM (0.666 μg/ml).

A different pharmacokinetic profile of the 2′,2′-difluoro-deoxyuridine was demonstrated for L-GEM (Fig. 6). The metabolite pharmacokinetic parameters were also different for free GEM, i.e., a C_{max} and $t_{1/2}$ of 1.57 μg/ml and ~ 10 h were achieved for L-GEM, respectively (Table 2). In particular, the pharmacokinetic profile of 2′,2′-difluorode-oxyuridine following L-GEM administration showed a plasma concentration increase up to 2 h, when the maximum metabolite concentration was measured, and a gradual decrease up to 24 h. The 2′,2′-difluorodeoxyuridine plasma concentration remained elevated (≥ 0.3 μg/ml) up to 16 h and a significant concentration was still determined in the plasma after 24 h (Fig. 6). Also in this case, these results were confirmed by the analysis of the V_d and AUC values. The metabolite derived from L-GEM showed an AUC value (23.302 μg/ml) ~ 2.2-fold higher than that obtained for the free GEM (10.26 μg/ml), while the V_d values of the two formulations were similar.

Fig. 4 In vivo antitumor effects of GEM (15 mg/kg) and L-GEM (5 mg/kg) against PC xenografts (**a**, **b**). CB-17 SCID-mice bearing PSN-1 and BxPC-3 xenografts cancer were i.p. treated twice a week for 5 weeks. Mouse survival following treatments are shown in **c** and **d**. Symbols: *filled circles* control; *filled triangles* treatment with unloaded liposomes; *filled squares* treatment with GEM; *filled diamonds* treatment with L-GEM. *P value refers to L-GEM versus GEM
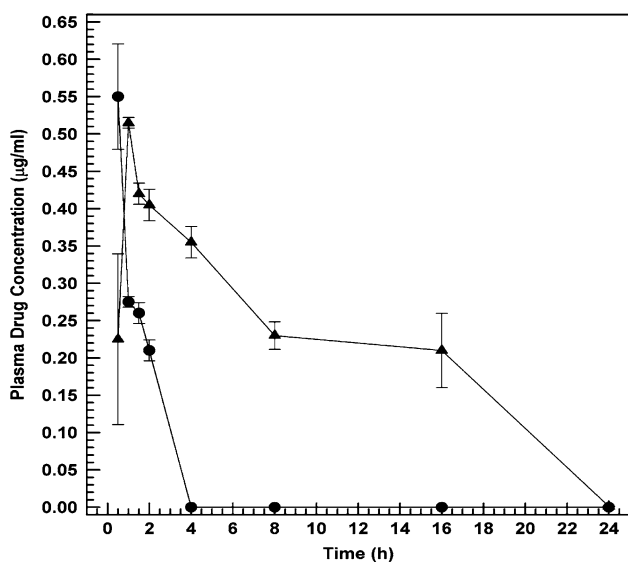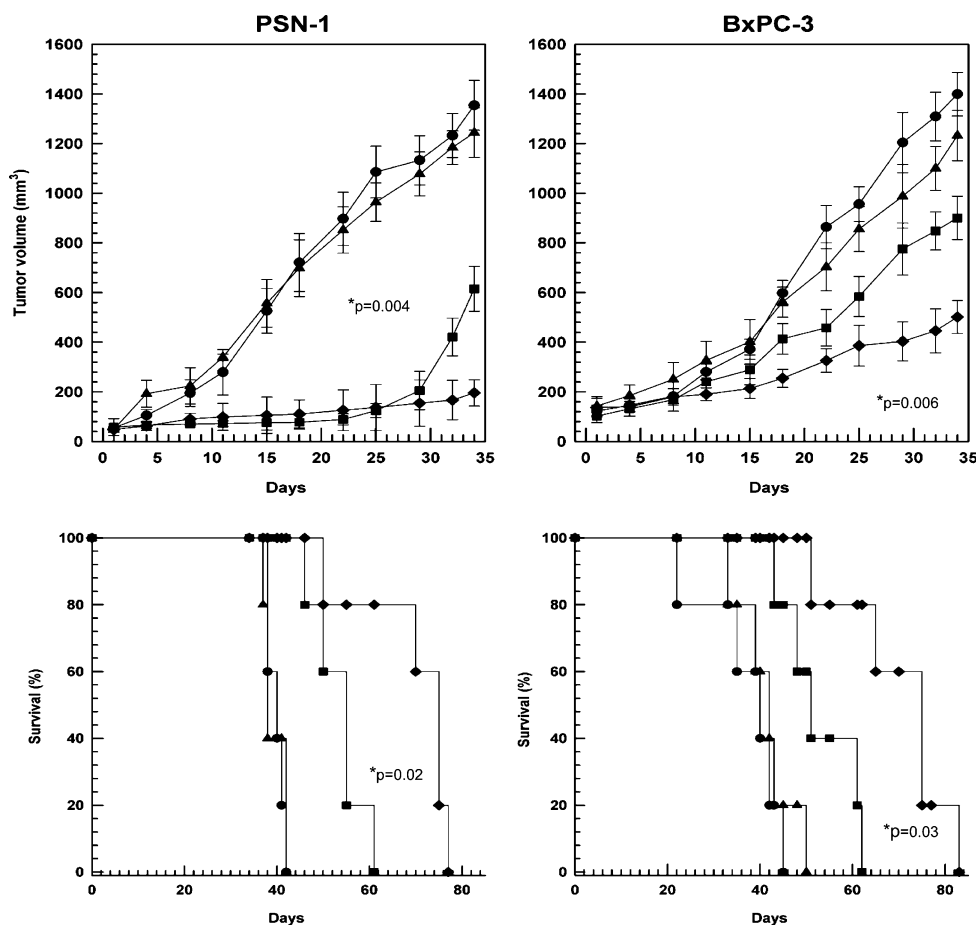

Fig. 5 Pharmacokinetic profile of free GEM (*filled circles*) and L-GEM (*filled triangles*) in CB-17 SCID-mice following i.v. administration (0.1 mg/mouse). Data are the average of three independent experiments ± standard deviation. The L-GEM profile was significantly different from that of GEM, ANOVA $P < 0.001$

Discussion

PC is a challenging disease for the modern oncology. While, localized and the locally advanced disease may benefit from surgery, radiation therapy and chemotherapy, the systemic treatment has only a palliative role in the advanced disease [25]. At present the conventional chemotherapy is based on GEM, which has a low toxicity profile, a short plasma half-life and a rapid inactivation by plasmatic enzymes, which may significantly affect the therapeutic potential of the drug.

A variety of approaches have been previously proposed to overcome the short half-life and increase bioavailability of GEM. Specifically, the conjugation with biocompatible materials [26–28] or the encapsulation within innovative colloidal drug delivery systems [29–31] have been investigated with the aim to modulate the biopharmaceutical properties of L-GEM. However, liposomes, which are commonly used in cancer treatment, still appear the most reliable drug delivery system for rapid translational purposes.

Table 2 Plasma pharmacokinetic parameters of GEM and its inactive metabolite, $2',2'$-difluorodeoxyuridine, after a single intravenous administration in CB-17 SCID-mice

Analysis	$t_{1/2}$ (h)	C_{max} (µg/ml)	T_{max} (h)	V_d (ml)	AUC (µg/ml h)
Free GEM	1.0 ± 0.12	0.55 ± 0.07	0.5 ± 0.1	181.81 ± 0.09	0.666 ± 0.034
L-GEM*	8.0 ± 0.26	0.51 ± 0.01	1.0 ± 0.1	444.44 ± 0.13	5.171 ± 0.029
Metabolite from GEM	4.0 ± 0.24	1.25 ± 0.05	0.5 ± 0.2	80.00 ± 0.20	10.260 ± 0.086
Metabolite from L-GEM*	10.0 ± 0.39	1.57 ± 0.08	2.0 ± 0.1	72.46 ± 0.11	23.302 ± 0.076

* All data of pharmacokinetic parameters have a statistical significance ANOVA $P < 0.001$ with respect to free GEM and metabolite from GEM
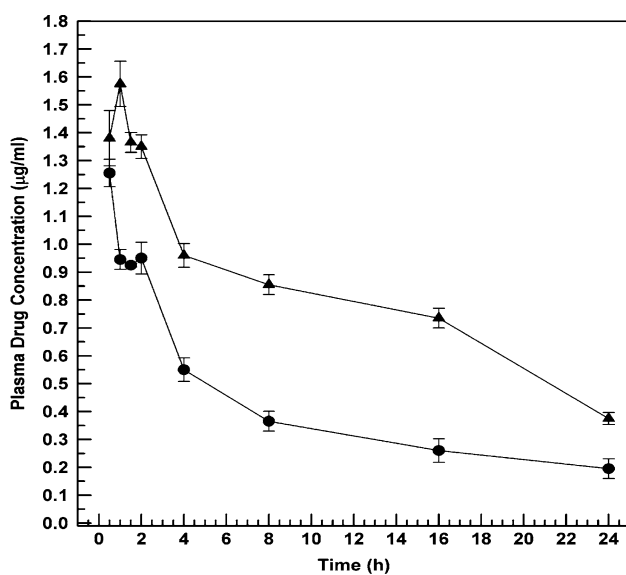

Fig. 6 Pharmacokinetic profile of the GEM inactive metabolite, $2',2'$-difluorodeoxyuridine, following free GEM (*filled circles*) and L-GEM (*filled triangles*) i.v. injection in CB-17 SCID-mice (0.1 mg/mouse). Data are the average of three independent experiments ± standard deviation. The L-GEM profile was significantly different from that of GEM, ANOVA $P < 0.001$

We previously reported that our original formulation of L-GEM disclosed in vitro antiproliferative activity against anaplastic thyroid cancer, multiple myeloma and colon carcinoma cell lines [15, 30, 32]. These preliminary investigations were however limited only to in vitro studies.

Here, we report that L-GEM fulfills two fundamental technological requirements to be an effective in vivo delivered drug: (1) an effective drug loading capacity of liposomes, which are useful to deliver a reasonable drug amount, and (2) a small ($\sim$100 nm) mean size, which is useful to achieve extravasation in the tumor microenvironment. In vitro cell growth studies on BxPC-3 and PSN-1 cell lines demonstrated that L-GEM significantly affected cell proliferation potential as compared to the free drug as shown by lower IC_{50} values. Moreover, CLSM experiments showed an efficient interaction of L-GEM with the cell membrane which suggest a greater drug internalization and activity as compared to free drug, in agreement with our previous observation [15]. Based on our data, the

endocytosis seems to be the most important mechanism of L-GEM internalization. It is important to consider that Doxil® (liposome formulation of doxorubicin), which did not show in vitro higher antiproliferative activity versus the free drug, then disclosed a significant therapeutic in vivo efficacy. This latter finding is probably due to the particular behavior of the liposome formulation and its lack of cardiac toxicity [33, 34].

On the bases of these considerations, we next assessed the pharmacokinetic and therapeutic activity of L-GEM in vivo versus the free GEM. To this end, BXPC-3 and PSN-1 xenografts in CB-17 SCID-mice were used to explore the antitumor activity of L-GEM. We indeed found higher in vivo antitumor activity of L-GEM as compared to the free drug which translated in a clear survival advantage of treated mice. Most importantly, this advantage was reached by administering only one-third of GEM dose entrapped in the liposomal carriers, suggesting therefore a higher therapeutic antitumor potential of L-GEM in vivo. These findings might be explained by differences of liposome features, which include: (1) protection of GEM from the plasmatic enzymes, (2) improvement of plasmatic half-life of GEM, and (3) an effective tumor targeting (EPR effect—passive targeting). The small size and the presence of PEG moieties along the surface of L-GEM allowed a long circulation time, as evidenced by the plasma levels. In fact, L-GEM disclosed a different pharmacokinetic versus GEM (Table 2). L-GEM disclosed a rapid plasmatic clearance after i.v. administration, probably due to the rapid enzymatic conversion into its inactive metabolite $2',2'$-difluorodeoxyuridine [29], while L-GEM is still present in plasma up to 24 h. The improvement of bioavailability of L-GEM was also confirmed by the AUC value, which was $\sim$7.5-fold higher than free GEM.

The different AUC, V_d and T_{max} parameters of L-GEM can be explained by a reduced metabolic inactivation of the drug entrapped in vesicular carrier. In fact, plasmatic levels of the inactive metabolite $2',2'$-difluorodeoxyuridine, produced by the catabolic effect of cytidine deaminase, are prolonged from of L-GEM, indicating both a long time presence of the drug in the plasma, and the need of the active compound to be leaked from L-GEM in order to be

metabolized. Therefore, L-GEM has an increased plasma stability and this can explain the improved therapeutic activity of the drug.

Taken together, our results strongly suggest that L-GEM has a promising antitumor activity in vivo against PC. Our work provides a rationale for further development of L-GEM as an investigational new drug for clinical use.

References

1. Jemal A, Siegel R, Ward E, Hao Y, Xu J, Murray T, Thun MJ (2008) Cancer statistics, 2008. CA Cancer J Clin 58:71–96
2. Manegold C (2004) Gemcitabine (Gemzar) in non-small cell lung cancer. Expert Rev Anticancer Ther 4:345–360
3. Abbruzzese JL, Grunewald R, Weeks EA, Gravel D, Adams T, Nowak B, Mineishi S, Tarassoff P, Satterlee W, Raber MN et al (1991) A phase I clinical, plasma, and cellular pharmacology study of gemcitabine. J Clin Oncol 9:491–498
4. Moog R, Burger AM, Brandl M, Schuler J, Schubert R, Unger C, Fiebig HH, Massing U (2002) Change in pharmacokinetic and pharmacodynamic behavior of gemcitabine in human tumor xenografts upon entrapment in vesicular phospholipid gels. Cancer Chemother Pharmacol 49:356–366
5. Soloman R, Gabizon AA (2008) Clinical pharmacology of liposomal anthracyclines: focus on pegylated liposomal Doxorubicin. Clin Lymphoma Myeloma 8:21–32
6. Celano M, Schenone S, Cosco D, Navarra M, Puxeddu E, Racanicchi L, Brullo C, Varano E, Alcaro S, Ferretti E, Botta G, Filetti S, Fresta M, Botta M, Russo D (2008) Cytotoxic effects of a novel pyrazolopyrimidine derivative entrapped in liposomes in anaplastic thyroid cancer cells in vitro and in xenograft tumors in vivo. Endocr Relat Cancer 15:499–510
7. Harasym TO, Cullis PR, Bally MB (1997) Intratumor distribution of doxorubicin following i.v. administration of drug encapsulated in egg phosphatidylcholine/cholesterol liposomes. Cancer Chemother Pharmacol 40:309–317
8. Drummond DC, Meyer O, Hong K, Kirpotin DB, Papahadjopoulos D (1999) Optimizing liposomes for delivery of chemotherapeutic agents to solid tumors. Pharmacol Rev 51:691–743
9. Nagayasu A, Uchiyama K, Kiwada H (1999) The size of liposomes: a factor which affects their targeting efficiency to tumors and therapeutic activity of liposomal antitumor drugs. Adv Drug Deliv Rev 40:75–87
10. Gabizon AA, Shmeeda H, Zalipsky S (2006) Pros and cons of the liposome platform in cancer drug targeting. J Liposome Res 16:175–183
11. Hatakeyama H, Akita H, Ishida E, Hashimoto K, Kobayashi H, Aoki T, Yasuda J, Obata K, Kikuchi H, Ishida T, Kiwada H, Harashima H (2007) Tumor targeting of doxorubicin by anti-MT1-MMP antibody-modified PEG liposomes. Int J Pharm 342:194–200
12. Beduneau A, Saulnier P, Benoit JP (2007) Active targeting of brain tumors using nanocarriers. Biomaterials 28:4947–4967
13. Tassone P, Tagliaferri P, Cucinotto I, Lavecchia AM, Leone F, Pietragalla A, Salvino A, Barbieri V, Venuta S (2007) Pegylated
14. Minisini AM, Andreetta C, Fasola G, Puglisi F (2008) Pegylated liposomal doxorubicin in elderly patients with metastatic breast cancer. Expert Rev Anticancer Ther 8:331–342
15. Celia C, Calvagno MG, Paolino D, Bulotta S, Ventura CA, Russo D, Fresta M (2008) Improved in vitro anti-tumoral activity, intracellular uptake and apoptotic induction of gemcitabine-loaded pegylated unilamellar liposomes. J Nanosci Nanotechnol 8:2102–2113
16. Hwang RF, Yokoi K, Bucana CD, Tsan R, Killion JJ, Evans DB, Fidler IJ (2003) Inhibition of platelet-derived growth factor receptor phosphorylation by STI571 (Gleevec) reduces growth and metastasis of human pancreatic carcinoma in an orthotopic nude mouse model. Clin Cancer Res 9:6534–6544
17. Hylander BL, Pitoniak R, Penetrante RB, Gibbs JF, Oktay D, Cheng J, Repasky EA (2005) The anti-tumor effect of Apo2L/TRAIL on patient pancreatic adenocarcinomas grown as xenografts in SCID mice. J Transl Med 3:22
18. Tassone P, Gozzini A, Goldmacher V, Shammas MA, Whiteman KR, Carrasco DR, Li C, Allam CK, Venuta S, Anderson KC, Munshi NC (2004) In vitro and in vivo activity of the maytansinoid immunoconjugate huN901–N2′-deacetyl-N2′-(3-mercapto-1-oxopropyl)-maytansine against CD56+ multiple myeloma cells. Cancer Res 64:4629–4636
19. Neri P, Tagliaferri P, Di Martino MT, Calimeri T, Amodio N, Bulotta A, Ventura M, Eramo PO, Viscomi C, Arbitrio M, Rossi M, Caraglia M, Munshi NC, Anderson KC, Tassone P (2008) In vivo anti-myeloma activity and modulation of gene expression profile induced by valproic acid, a histone deacetylase inhibitor. Br J Haematol 143:520–531
20. Shimamura T, Royal RE, Kioi M, Nakajima A, Husain SR, Puri RK (2007) Interleukin-4 cytotoxin therapy synergizes with gemcitabine in a mouse model of pancreatic ductal adenocarcinoma. Cancer Res 67:9903–9912
21. Damaraju VL, Bouffard DY, Wong CK, Clarke ML, Mackey JR, Leblond L, Cass CE, Grey M, Gourdeau H (2007) Synergistic activity of troxacitabine (Troxatyl) and gemcitabine in pancreatic cancer. BMC Cancer 7:121
22. Heinemann V, Xu YZ, Chubb S, Sen A, Hertel LW, Grindey GB, Plunkett W (1992) Cellular elimination of 2′, 2′-difluorodeoxycytidine 5′-triphosphate: a mechanism of self-potentiation. Cancer Res 52:533–539
23. Bouffard DY, Laliberte J, Momparler RL (1993) Kinetic studies on 2′, 2′-difluorodeoxycytidine (Gemcitabine) with purified human deoxycytidine kinase and cytidine deaminase. Biochem Pharmacol 45:1857–1861
24. Matsuda A, Sasaki T (2004) Antitumor activity of sugar-modified cytosine nucleosides. Cancer Sci 95:105–111
25. Morgan MA, Parsels LA, Kollar LE, Normolle DP, Maybaum J, Lawrence TS (2008) The combination of epidermal growth factor receptor inhibitors with gemcitabine and radiation in pancreatic cancer. Clin Cancer Res 14:5142–5149
26. Wu W, Sigmond J, Peters GJ, Borch RF (2007) Synthesis and biological activity of a gemcitabine phosphoramidate prodrug. J Med Chem 50:3743–3746
27. Pasut G, Canal F, Dalla Via L, Arpicco S, Veronese FM, Schiavon O (2008) Antitumoral activity of PEG-gemcitabine prodrugs targeted by folic acid. J Control Release 127:239–248
28. Reddy LH, Couvreur P (2008) Novel approaches to deliver gemcitabine to cancers. Curr Pharm Des 14:1124–1137
29. Stella B, Arpicco S, Rocco F, Marsaud V, Renoir JM, Cattel L, Couvreur P (2007) Encapsulation of gemcitabine lipophilic derivatives into polycyanoacrylate nanospheres and nanocapsules. Int J Pharm 344:71–77

liposomal doxorubicin is active in Stewart-Treves syndrome. Ann Oncol 18:959–960

30. Celia C, Malara N, Terracciano R, Cosco D, Paolino D, Fresta M, Savino R (2008) Liposomal delivery improves the growth-inhibitory and apoptotic activity of low doses of gemcitabine in multiple myeloma cancer cells. Nanomedicine 4:155–166

31. Paolino D, Cosco D, Licciardi M, Giammona G, Fresta M, Cavallaro G (2008) Polyaspartylhydrazide copolymer-based supramolecular vesicular aggregates as delivery devices for anticancer drugs. Biomacromolecules 9:1117–1130

32. Calvagno MG, Celia C, Paolino D, Cosco D, Iannone M, Castelli F, Doldo P, Frest M (2007) Effects of lipid composition and preparation conditions on physical-chemical properties, technological parameters and in vitro biological activity of gemcitabine-loaded liposomes. Curr Drug Deliv 4:89–101

33. Rahman AM, Yusuf SW, Ewer MS (2007) Anthracycline-induced cardiotoxicity and the cardiac-sparing effect of liposomal formulation. Int J Nanomedicine 2:567–583

34. Verma S, Dent S, Chow BJ, Rayson D, Safra T (2008) Metastatic breast cancer: the role of pegylated liposomal doxorubicin after conventional anthracyclines. Cancer Treat Rev 34:391–406